Nuclear Engineering and Technology 55 (2023) 3080–3087

Contents lists available at ScienceDirect

Nuclear Engineering and Technology

journal homepage: www.elsevier.com/locate/net

Original Article

Neutron-irradiated effect on the thermoelectric properties of Bi_2Te_3-based thermoelectric leg

Huanyu Zhao [a, 1], Kai Liu [b, 1], Zhiheng Xu [a, c, *], Yunpeng Liu [a, c], Xiaobin Tang [a, c, **]

[a] Department of Nuclear Science and Technology, Nanjing University of Aeronautics and Astronautics, Nanjing, 211106, China
[b] State Key Laboratory of Silicon Materials, School of Materials Science and Engineering, Zhejiang University, Hangzhou, 310027, China
[c] Key Laboratory of Nuclear Technology Application and Radiation Protection in Astronautics, Ministry of Industry and Information Technology, Nanjing, 211106, China

ARTICLE INFO

Article history:
Received 14 October 2022
Received in revised form
30 March 2023
Accepted 25 April 2023

Keywords:
Neutron irradiation
Electrical conductivity
Thermoelectric
$Bi_2Te_{2.7}Se_{0.3}$
$Bi_{0.5}Sb_{1.5}Te_3$

ABSTRACT

Thermoelectric (TE) materials working in radioisotope thermoelectric generators are irradiated by neutrons throughout its service; thus, investigating the neutron irradiation stability of TE devices is necessary. Herein, the influence of neutron irradiation with fluences of 4.56×10^{10} and 1×10^{13} n/cm^2 by pulsed neutron reactor on the electrical and thermal transport properties of n-type $Bi_2Te_{2.7}Se_{0.3}$ and p-type $Bi_{0.5}Sb_{1.5}Te_3$ thermoelectric alloys prepared by cold-pressing and molding is investigated. After neutron irradiation, the properties of thermoelectric materials fluctuate, which is related to the material type and irradiation fluence. Different from p-type thermoelectric materials, neutron irradiation has a positive effect on n-type $Bi_2Te_{2.7}Se_{0.3}$ materials. This result might be due to the increase of carrier mobility and the optimization of electrical conductivity. Afterward, the effects of p-type and n-type TE devices with different treatments on the output performance of TE devices are further discussed. The positive and negative effects caused by irradiation can cancel each other to a certain extent. For TE devices paired with p-type $Bi_{0.5}Sb_{1.5}Te_3$ and n-type $Bi_2Te_{2.7}Se_{0.3}$ thermoelectric legs, the generated power and conversion efficiency are stable after neutron irradiation.

1. Introduction

Radioisotope thermoelectric generators (RTGs) are the main power source, or even the only power source, for current deep space exploration missions [1,2]. To date, RTGs have been used in space missions for many times. They are not affected by sunlight, weather, and dust, and they have stable output power, high energy density, long service life, and mature technology. For example, the Curiosity rover that landed on Mars in 2011 used 110 W multi-mission RTGs, which have been working normally for more than 10 years, supporting the rover to explore waters, climate, and geological changes of Mars [3]. In addition, micro-RTGs can be used to drive scientific instruments to explore extraterrestrial planets, and the RTGs are approximately 4.3 cm^3 in size, which possess more than 450 μW of power [4,5].

The general structure of the RTG is primarily composed of three parts: heat source, thermoelectric conversion device, and radiator. Thermoelectric conversion devices are the core components for the direct conversion of thermal energy into electrical energy by Seebeck effect. The performance of thermoelectric materials and their device is critical to RTG output. Current research on materials and devices primarily focuses on thermoelectric performance improvement and stability. The thermoelectric characteristics of RTGs can meet the needs of engineering applications, particularly in aerospace engineering. With the deepening of application research, their service stability becomes increasingly important. Stability research primarily focuses on the thermal stability, irradiation stability, and mechanical stability of thermoelectric materials and devices, such as high temperature, α particles, neutrons, protons, and toughness [6–11]. Among them, neutrons are produced by the isotope heat source, which have high penetration that could affect materials and devices. Studies have shown that the type of thermoelectric material, neutron irradiation dose,

* Corresponding author. Department of Nuclear Science and Technology, Nanjing University of Aeronautics and Astronautics, Nanjing, 211106, China.
** Corresponding author. Department of Nuclear Science and Technology, Nanjing University of Aeronautics and Astronautics, Nanjing, 211106, China.
E-mail addresses: xuzhiheng@nuaa.edu.cn (Z. Xu), tangxiaobin@nuaa.edu.cn (X. Tang).
[1] These authors contributed to the work equally and should be regarded as co-first authors.

https://doi.org/10.1016/j.net.2023.04.036

irradiation temperature, and other factors affect the performance of thermoelectric materials after neutron irradiation, that is, the performance of thermoelectric materials under different neutron irradiation conditions is complicated [9–11]. Neutrons can affect grain boundary and material structure, and then the properties of it change [12–14]. It is reported that neutrons have an important impact on semiconductor materials [15–18], especially in thermal conductivity and electrical conductivity which are the noteworthy factors affecting the performance of thermoelectric materials [19–23]. Based on existing studies, in RTGs, the cumulative neutron fluence of TE devices during service is less than 10^{12} n/cm^2 magnitude [9]. Previous research has studied the effect of neutron fluence at 1.3 × 10^{18} n/cm^2 on n-type $Bi_2Te_{2.7}Se_{0.3}$ and p-type $Bi_{0.5}Sb_{1.5}Te_3$ materials, which indicates that the power factor of n-type $Bi_2Te_{2.7}Se_{0.3}$ thermoelectric materials and the thermal conductivity of p-type $Bi_{0.5}Sb_{1.5}Te_3$ materials increase [11]. Changes in materials such as electric transport performance and thermal transport performance caused by neutron irradiation during service life directly influence the output and longevity of the device [24]. Therefore, studying the overall performance variation of the device under neutron irradiation is necessary. In addition, the neutron irradiation stability of the device must be tested when exploring new preparation process, new structure composition, and new combination mode.

In this work, the neutron irradiation stability of thermoelectric materials and devices using experimental and simulation methods was investigated. Based on the existing research results, representative thermoelectric materials such as n-type $Bi_2Te_{2.7}Se_{0.3}$ and p-type $Bi_{0.5}Sb_{1.5}Te_3$ bulk materials at a low temperature range were selected as the research object. In addition to the unirradiated control group, the irradiation neutron total fluence of 4.56 × 10^{10} n/cm^2 (defined as low fluence) and 1 × 10^{13} n/cm^2 (defined as high fluence) were added to verify the effects of neutron irradiation and its fluence. After testing the thermoelectric properties of n-type $Bi_2Te_{2.7}Se_{0.3}$ and p-type $Bi_{0.5}Sb_{1.5}Te_3$ materials with and without neutron irradiation, a finite-element simulation was used to study the stability of the TE device paired with p-type $Bi_{0.5}Sb_{1.5}Te_3$ and n-type $Bi_2Te_{2.7}Se_{0.3}$ thermoelectric legs.

2. Experimental sections

2.1. Experimental methods

As shown in Fig. 1, the bulk materials that be irradiated were prepared by cold-press sintering and molding [25]. First, thermoelectric paints composed of commercial Bi_2Te_3-based alloy (n-type: $Bi_2Te_{2.7}Se_{0.3}$, p-type: $Bi_{0.5}Sb_{1.5}Te_3$, Chengdu alfa metal) powder blended with DER732 binder (polypropylene glycol diglycidyl ether, Aladdin) were placed into the mold. Second, pressure was applied to the filled mold by using a press machine to enhance the tightness of the alloy. Then, they were demolded and sintered at 573.15 K for 3.5 h. After forming the slices, corresponding neutron irradiation experiments were conducted. Our neutron irradiation test was carried out in a Xi'an pulsed neutron reactor. The neutron flux produced by reactor is 1.7× 10^9 n/cm^2·s, the neutrons have an energy range of 0–10 MeV, average energy is 2.1 MeV, and the irradiation temperature was maintained at 300 K.

2.2. Characterization of thermoelectric materials

For thermoelectric materials, the dimensionless TE figure of merit is an important evaluation factor, as given by Eq. (1), which is primarily associated with Seebeck coefficient (S), electrical conductivity (σ), and thermal conductivity (κ). The Seebeck coefficient can be used to characterize the magnitude of the Seeback effect. As shown in Eq. (2), S is related to the carrier concentration (n) and effective mass (m^*) of the material. It is to be hoped that the internal resistance of material would be small in order to generate more electricity, so the electrical conductivity has an impact on thermoelectric material. σ is proportional to the carrier concentration and carrier mobility (μ). It is earnestly hoped that the temperature difference between the ends of the thermoelectric material is large, so the thermal conductivity of thermoelectric material is also important. κ is primarily composed of two parts: lattice thermal conductivity (κ_L) and electronic thermal conductivity (κ_e). Based on Eq. (1), an excellent thermoelectric material usually has a large Seebeck coefficient, high electrical conductivity, and low thermal conductivity.

$$ZT = \frac{S^2\sigma}{\kappa}T, \tag{1}$$

$$S = \frac{8\pi^2 k_B^2 T}{3eh^2} m^* \left(\frac{\pi}{3n}\right)^{2/3}, \tag{2}$$

$$\sigma = ne\mu, \tag{3}$$

$$\kappa = \kappa_L + \kappa_e, \tag{4}$$

where T is absolute temperature, e is the carrier charge, k_B is the Boltzmann constant, h is the Planck constant. S and σ were obtained using Cryoall CTA under argon atmosphere between 300 K and 700 K. κ was obtained using LFA500 under nitrogen atmosphere between 300 K and 550 K. Carrier concentration and Hall mobility were obtained using the Hall effect testing system (HT-50 type) at room temperature. The size of all test samples was set to 10 mm × 6.7 mm × 1.5 mm.

2.3. Finite element analysis

The effect of neutron irradiation on the properties of the Bi_2Te_3-based TE device was simulated by finite element method using COMSOL Multiphysics. The thermoelectric parameters of S, σ, and κ for the p/n-type materials with and without irradiation were fed into the model. After simulation, heat flux, output power, and other output data were generated [25]. The model structure of the TE device is illustrated in the subsequent part. The dimension of n-type and p-type thermoelectric leg was 4 mm × 4 mm × 3 mm. The spacing between the thermoelectric legs was set to 1 mm. Hot and cold side temperatures were defined as 300 K and 550 K respectively.

3. Results and discussions

3.1. Thermoelectric properties of n-type $Bi_2Te_{2.7}Se_{0.3}$ and p-type $Bi_{0.5}Sb_{1.5}Te_3$ materials

The performance curves of the n-type $Bi_2Te_{2.7}Se_{0.3}$ materials with or without neutron irradiation are presented in Fig. 2. Interestingly, the n-type thermoelectric legs are optimized after neutron irradiation modification. Fig. 2(a) shows the change in temperature of the Seebeck coefficient of n-type materials before and after neutron irradiation. Regardless of the treatment the n-type material receives, the variation law of S with temperature is almost the same. The Seebeck coefficient reaches its maximum value with the increase of temperature and then declines because of the presence of minority carriers (holes) with positive Seebeck coefficients [26]. The Seebeck coefficient of materials varies between −104 and −184 μV/K. That is, neutron irradiation has little effect on the

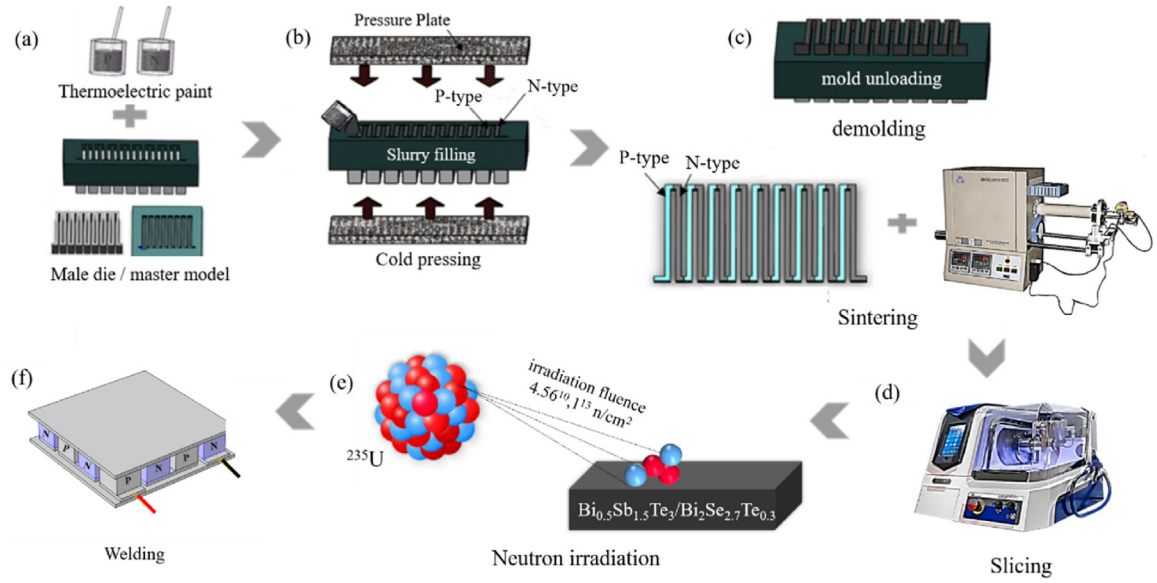

Fig. 1. Preparation process based on cold-press sintering and molding.

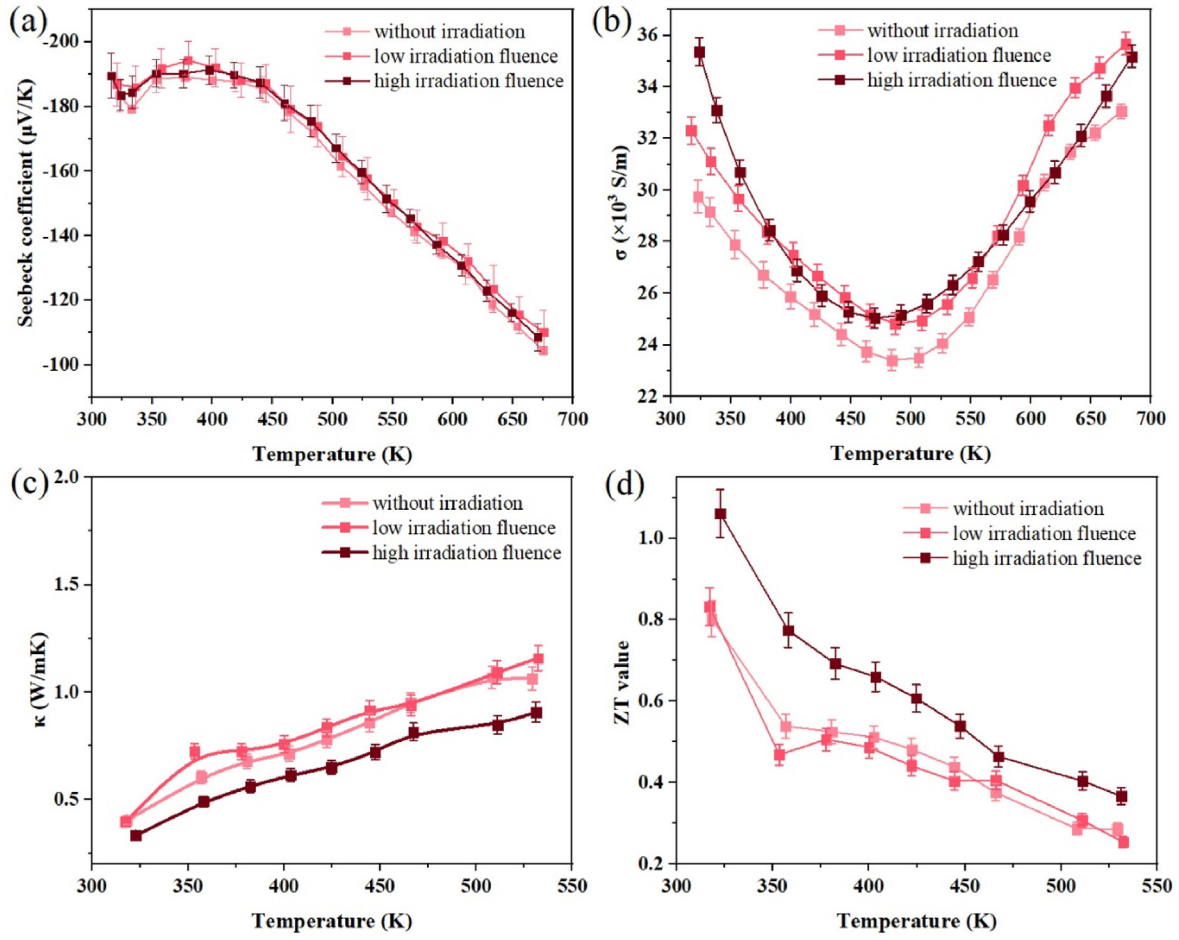

Fig. 2. Thermoelectric parameters of n-type $Bi_2Te_{2.7}Se_{0.3}$ materials before and after neutron irradiation: (a) Seebeck coefficient, (b) electrical conductivity, (c) thermal conductivity, and (d) figure of merit.

Seebeck coefficient of n-type $Bi_2Te_{2.7}Se_{0.3}$. The enhancement of electrical properties of materials by neutron irradiation is primarily reflected in the increase of electrical conductivity. As shown in Fig. 2(b), the electrical conductivity of neutron-irradiated n-type $Bi_2Te_{2.7}Se_{0.3}$ materials can reach 32.31×10^3 and 35.37×10^3 S/m at 322 K, whereas that of non-irradiated n-type thermoelectric

materials is 29.75 × 10^3 S/m. Within the working temperature range of n-type $Bi_2Te_{2.7}Se_{0.3}$ materials, the electrical conductivity of n-type $Bi_2Te_{2.7}Se_{0.3}$ materials increases by 6.4% after low neutron irradiation fluence and 8.2% after high neutron irradiation fluence. At 300 K–375 K, the electrical conductivity at high fluence increases greatly, which indicates that high-fluence neutron irradiation has a stronger effect on materials at low temperature. At low fluence, the thermal conductivity slightly changes, but the thermal conductivity changes remarkably under high fluence conditions, with an average decrease of 16.6%, as shown in Fig. 2(c). Fig. 2(d) shows that the ZT values of the irradiated n-type $Bi_2Te_{2.7}Se_{0.3}$ thermoelectric materials are higher than those of the unirradiated materials. The ZT value is maximum at approximately 320 K, which decreases with the increase of temperature. The maximum and average ZT value of n-type $Bi_2Te_{2.7}Se_{0.3}$ materials increase by 32.1% and 31.1%, respectively, after high-fluence neutron irradiation.

However, contrary to n-type $Bi_2Te_{2.7}Se_{0.3}$ materials, the Seebeck coefficient and electrical conductivity of p-type $Bi_{0.5}Sb_{1.5}Te_3$ materials decrease after neutron irradiation. As shown in Fig. 3(a), the fluctuation of the Seebeck coefficient of p-type $Bi_{0.5}Sb_{1.5}Te_3$ materials is relatively smooth under different neutron irradiation conditions; the three curves are not much apart, and the changes are primarily concentrated in the range of 300 K–450 K. The Seebeck coefficient of three p-type thermoelectric materials varies roughly within 112–206 μV/K, and its variation is greater than that of n-type materials. Comparing the electrical conductivity before and after neutron irradiation, neutron irradiation greatly affects the electrical conductivity of p-type materials, as shown in Fig. 3 (b). The electrical conductivity of the materials was dropped from 28.20 × 10^3 to 23.95 × 10^3 S/m at room temperature. The electrical conductivity of p-type $Bi_{0.5}Sb_{1.5}Te_3$ materials decreases by 11.4% after neutron irradiation fluence of 4.56 × 10^{10} n/cm^2 and by 14.5% after neutron irradiation fluence at 1 × 10^{13} n/cm^2. Consistent with n-type material, the electrical conductivity of p-type material decreases firstly and then increases as temperature increases. To start with, as temperature increases, lattice vibration intensifies, resulting in carrier scattering then decreasing carrier mobility and the electrical conductivity. When the intrinsic excitation temperature is reached, the carriers in the material are excited, which increases the carrier concentration and makes the electrical conductivity rises again. It is reported that neutron irradiation creates point defects and defect clusters could also be affected by annealing in materials [11], so the electrical conductivity increases at high temperature might due to the annealing and excitation of the material. Fig. 3(c) shows that the thermal conductivity of the p-type $Bi_{0.5}Sb_{1.5}Te_3$ material does not change much (from 0.47 to 0.46 W/mK at 317 K) before and after irradiation, which indicates that low- and high-fluence neutron irradiation has little effect on the thermal conductivity of p-type materials. As shown in Fig. 3(d), the maximum and average ZT values of p-type $Bi_{0.5}Sb_{1.5}Te_3$ materials decreased by 24.1% and 10.4% after neutron irradiation of 4.56 × 10^{10} n/cm^2, and decreased by 24.3% and 19.9% after neutron

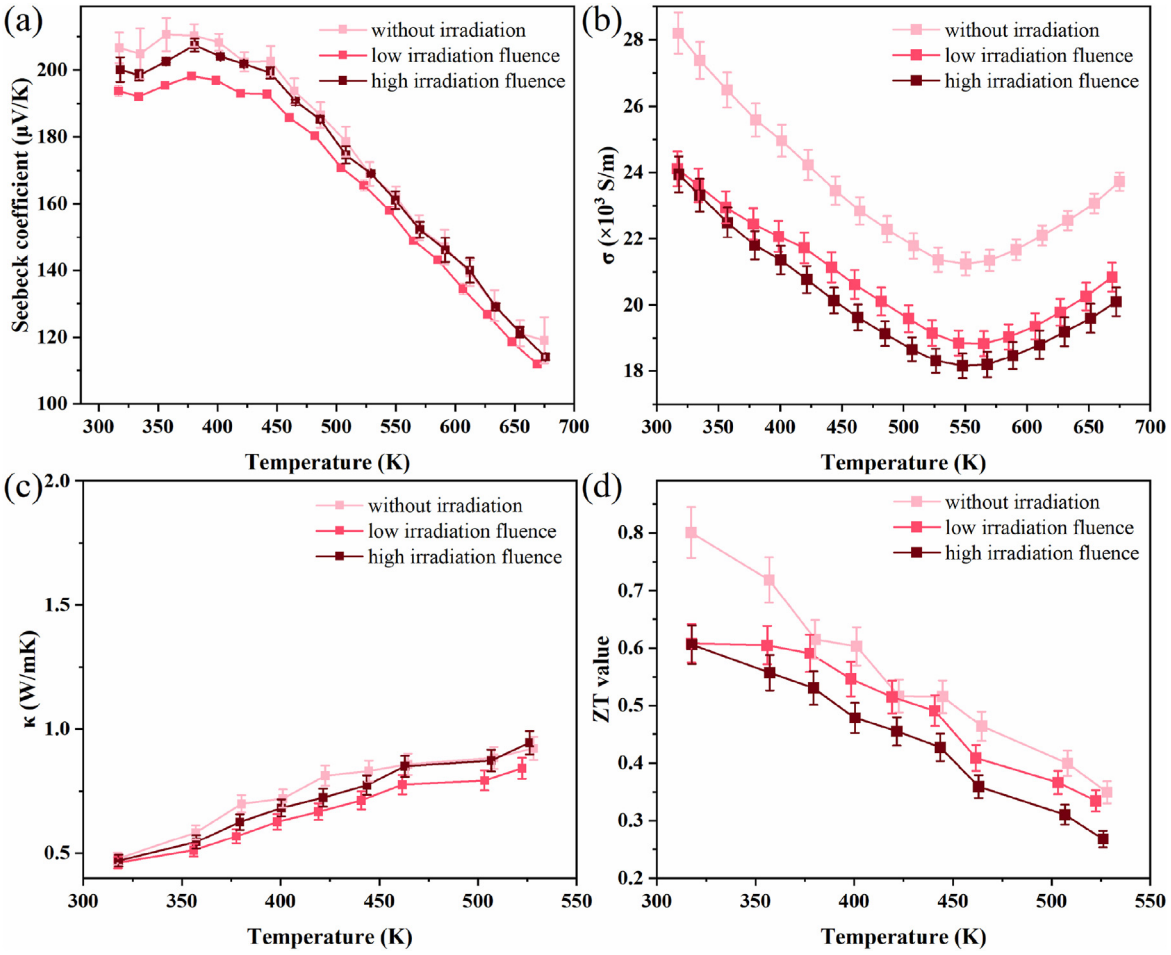

Fig. 3. Thermoelectric parameters of p-type bismuth telluride materials before and after neutron irradiation: (a) Seebeck coefficient, (b) electrical conductivity, (c) thermal conductivity, and (d) figure of merit.

irradiation of 1×10^{13} n/cm^2, respectively.

In general, in obtaining large heat to electricity conversion efficiency, the thermoelectric material must have a good Seebeck coefficient and electrical conductivity to transport electricity and a poor thermal conductivity to maintain a temperature difference. After irradiation, the electrical conductivity of the n-type $Bi_2Te_{2.7}Se_{0.3}$ material increases and decreases in p-type $Bi_{0.5}Sb_{1.5}Te_3$ materials, which changes their ZT value accordingly. The difference between n-type $Bi_2Te_{2.7}Se_{0.3}$ and p-type $Bi_{0.5}Sb_{1.5}Te_3$ under neutron irradiation was further analyzed from the internal mechanism. The changes in n-type $Bi_2Te_{2.7}Se_{0.3}$ and p-type $Bi_{0.5}Sb_{1.5}Te_3$ material carrier transport properties before and after neutron irradiation are shown in Table 1. The Seebeck coefficient is proportional to the effective mass and inversely proportional to $n^{2/3}$, and the effective mass and carrier concentration of the n-type material decrease after irradiation. Thus, the Seebeck coefficient slightly changes before and after irradiation. The enhancement of electrical conductivity is primarily due to the increase of carrier mobility, as the electrical conductivity is proportional to carrier mobility. The semiclassical Mott–Jones formula (Eq. (2)) shows that the Seebeck coefficient and carrier concentration can be estimated as $S \sim n^{-2/3}$ [27]. However, the measured S value for bulk materials with and without irradiation do not conform to this law, indicating that other factors such as potential-barrier scattering may play an important role in affecting n. Notably, the potential barriers at the interfaces and grain boundaries can filter low-energy carriers, which can decrease carrier concentration and enhance carrier mobility [28–30]. The other notable attraction is the ubiquitous lattice strain in the grain boundaries, which causes strong scattering of phonons, reducing thermal conductivity [31]. These phenomena correspond to the changes in the properties of n-type materials caused by neutron irradiation; thus, the change in grain boundaries produced by neutron irradiation increases the ZT value in n-type materials. Notably, the hall mobility of p-type $Bi_{0.5}Sb_{1.5}Te_3$ materials shows evident decrease, and carrier concentration increases after irradiation. Irradiation-induced point defects in $Bi_{0.5}Sb_{1.5}Te_3$ materials, such as vacancies, substantially reduce charge carrier mobility via local charge order, which affect the thermoelectric properties of p-type $Bi_{0.5}Sb_{1.5}Te_3$ materials [32,33].

Although the substrate crystal structure is the same, the p-type $Bi_{0.5}Sb_{1.5}Te_3$ material is insensitive to thermal irradiation compared with n-type $Bi_2Te_{2.7}Se_{0.3}$. The T dependent σ(T) is usually used to judge the scattering mechanism. The acoustic phonon scattering is usually the dominant carrier scattering mechanisms for heavily doped thermoelectric semiconductors, giving a negative T-dependence. When grain boundary scattering plays an important or even dominant role in the carrier transport, σ(T) usually tends to rise with positive T-dependence [34]. Therefore, in the temperature range of our interest, 300–550 K, for n-type materials, the main scattering mechanism is acoustic phonon scattering in the range of 300–470 K, and grain boundary scattering in the range of 470–550 K, and the main scattering mechanism is acoustic phonon scattering in the range of 300–550 K for p-type materials. It is reported that when the grain size is much smaller than the mean free path of phonons, phonons are almost not scattered [35], therefore, based on the experimental results that defects introduced in n-type materials having a scattering effect on phonons, whereas defects introduced in p-type materials have little effect on phonons, we believe that, the neutron irradiation has almost no effect on the size of p-type materials, but increasing the size of n-type materials which enhances phonon scattering in n-type materials. For materials that the main scattering mechanism is grain boundary scattering, smaller grains in nanoscale thermoelectric materials generally lead to a decrease in thermal conductivity through grain boundary scattering. The grain size of the material can be changed by hydrothermal method during preparing or by spark plasma sintering during sintering [36–40], thereby when the main scattering mechanisms in the material determines, the thermal conductivity can be optimized by adjusting the grain size. Furthermore, measures such as radiation hardening in p-type $Bi_{0.5}Sb_{1.5}Te_3$ materials must be observed to maintain its decent performance.

3.2. Thermoelectric properties of n-type $Bi_2Te_{2.7}Se_{0.3}$ and p-type $Bi_{0.5}Sb_{1.5}Te_3$ devices

COMSOL simulation was used to study the power and efficiency changes of thermoelectric legs with a certain temperature difference and deeply analyze the influence of neutron irradiation on TE devices. The obtained distribution of temperature (T) and electrical potential (ϕ) of n-type $Bi_2Te_{2.7}Se_{0.3}$ and p-type $Bi_{0.5}Sb_{1.5}Te_3$ single leg is given in Figs. 4 and 5, respectively. Given the high Seebeck coefficient of p-type $Bi_{0.5}Sb_{1.5}Te_3$ leg, its open-circuit voltage is higher than that of n-type $Bi_2Te_{2.7}Se_{0.3}$ leg at the same temperature difference (250 K) [26].

The output characteristics of n-type $Bi_2Te_{2.7}Se_{0.3}$ and p-type $Bi_{0.5}Sb_{1.5}Te_3$ thermoelectric legs are shown in Table 2. Before irradiation, the p-type thermoelectric legs have higher open-circuit voltage, lower internal resistance, and therefore higher power generation. The internal resistance and conductivity of the thermoelectric legs change after irradiation, which makes output power different. When the open-circuit voltage is similar and the internal resistance is small, the corresponding output power and conversion efficiency are high [41]. After neutron irradiation, the open-circuit voltage of the p-type $Bi_{0.5}Sb_{1.5}Te_3$ thermoelectric leg decreases, and the internal resistance increases. Thus, the output power decreases, and the conversion efficiency drops from 6.25% to 5.74% at a low neutron irradiation fluence and 5.24% at a high fluence. The n-type thermoelectric leg has the opposite effect of the p-type. The open-circuit voltage of the n-type $Bi_2Te_{2.7}Se_{0.3}$ TE leg increases; the internal resistance decreases; the output power is

Table 1
Electronic transport properties with respect to neutron irradiation fluence at 300 K.

Parameter	Value					
Type of TE material	n-$Bi_2Te_{2.7}Se_{0.3}$			p-$Bi_{0.5}Sb_{1.5}Te_3$		
	Without irradiation	Low-fluence irradiation	High-fluence irradiation	Without irradiation	Low-fluence irradiation	High-fluence irradiation
Carrier concentration ($\times 10^{19}$ cm^{-3})	9.19	4.18	1.52	3.14	4.08	20.57
Hall mobility (cm^3 V^{-1} s^{-1})	9.17	20.24	45.14	15.89	12.27	2.33
Seebeck coefficient (μV/K)	−183.51	−186.80	−189.48	206.69	194.77	197.55
Electrical conductivity ($\times 10^3$ S/m)	29.75	32.31	35.37	28.20	24.11	23.95
Effective mass[a] (m_0)	2.56	1.53	0.81	1.54	1.68	4.97

[a] m_0 is the free electron rest mass.

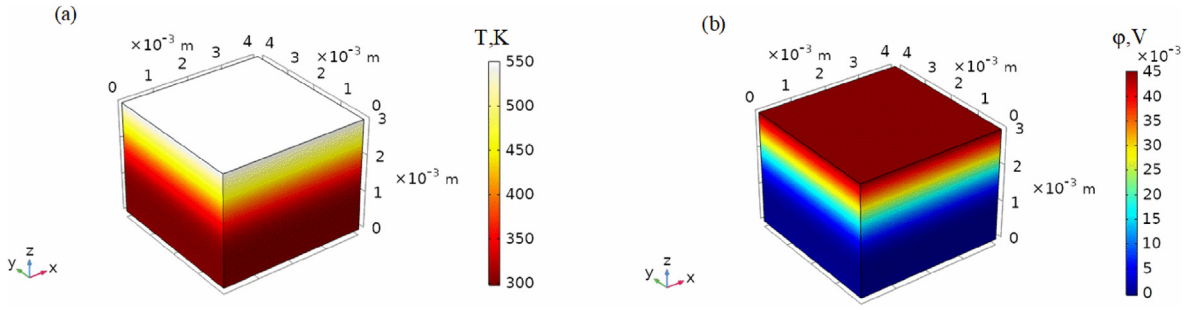

Fig. 4. (a) Temperature and (b) electrical potential distribution of n-type $Bi_2Te_{2.7}Se_{0.3}$ thermoelectric leg.

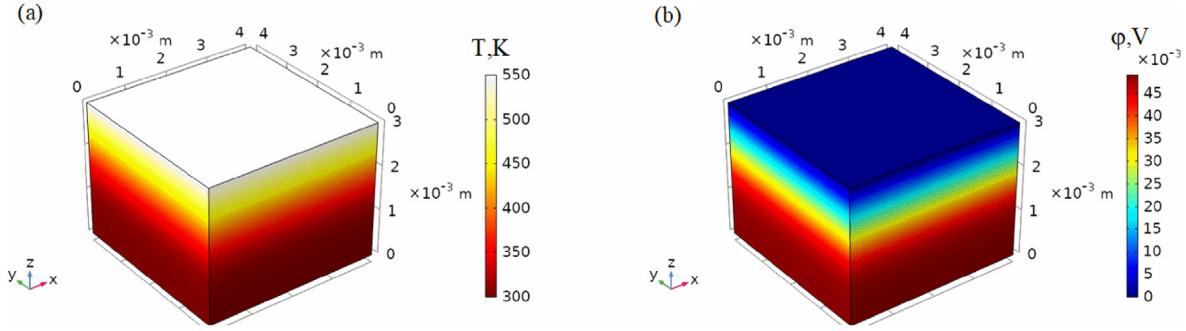

Fig. 5. (a) Temperature and (b) electrical potential distribution of p-type $Bi_{0.5}Sb_{1.5}Te_3$ thermoelectric leg.

Table 2
Output characteristics of the thermoelectric leg at a temperature difference of ΔT = 250 K (T_h = 550 K, T_c = 300 K).

Parameter	Value					
Type of TE material	n-$Bi_2Te_{2.7}Se_{0.3}$			p-$Bi_{0.5}Sb_{1.5}Te_3$		
	Without irradiation	Low-fluence irradiation	High-fluence irradiation	Without irradiation	Low-fluence irradiation	High-fluence irradiation
Open-circuit voltage, V_{oc} (mV)	44.41	45.22	45.04	49.10	46.57	46.57
The internal resistance, R (mΩ)	4.11	3.86	3.42	3.94	3.86	4.23
Generated power, P (mW)	120.0	132.4	148.3	152.9	140.4	128.2
Current, I across the leg (A)	5.4	5.9	6.6	6.2	6.0	5.5
Efficiency, η	5.51%	6.08%	6.81%	6.25%	5.74%	5.24%

improved, and the efficiency increases from 5.88% to 6.08% at a low irradiation fluence and 6.81% at a high fluence. These results are consistent with the previous effect of n-type $Bi_2Te_{2.7}Se_{0.3}$ material performance enhancement, and the performance of p-type $Bi_{0.5}Sb_{1.5}Te_3$ materials decrease after neutron irradiation, which indicates that neutron irradiation affects the output and efficiency performance of n-type $Bi_2Te_{2.7}Se_{0.3}$ and p-type $Bi_{0.5}Sb_{1.5}Te_3$ materials.

Considering that the TE device is paired with p-type and n-type thermoelectric legs, a post-irradiation performance evaluation of

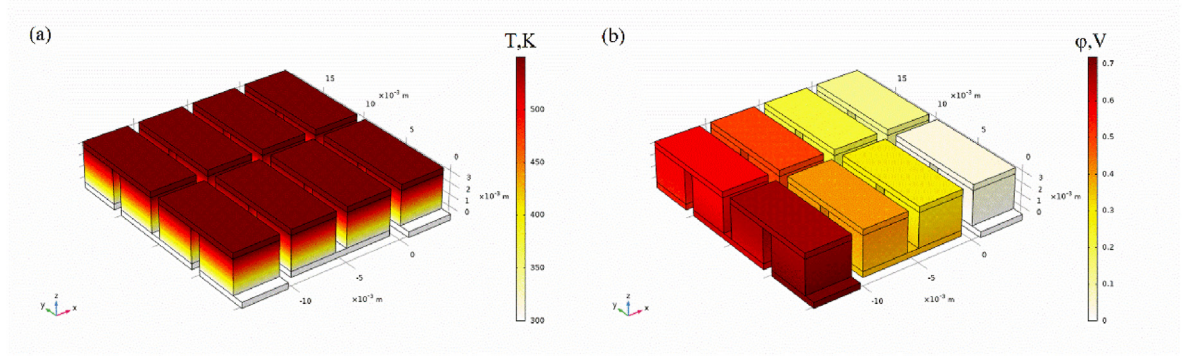

Fig. 6. (a) Temperature and (b) electrical potential distribution of eight pairs of Bi_2Te_3-based devices.

Table 3
Output characteristics of eight pairs of Bi_2Te_3-based devices at $T_h = 550$ K and $T_c = 300$ K.

Parameter	Value			
Type of TE device	p-without irradiation + n-without irradiation	p-low irradiation fluence + n-low irradiation fluence	p-high irradiation fluence + n-high irradiation fluence	p-without irradiation + n-high irradiation fluence
Output voltage, V_{oc} (mV)	735.27	722.00	720.47	740.26
The internal resistance, R (mΩ)	64.40	61.76	61.20	58.88
Generated power, P (mW)	2098.7	2110.1	2120.4	2326.7
Efficiency, η	5.88%	5.91%	5.94%	6.53%

the p- and n-combined device must be performed. The obtained T and ϕ distributions of the eight pairs of Bi_2Te_3-based devices are shown in Fig. 6. Compared with thermoelectric single leg, the temperature distribution of the TE device is more uniform under the thermal conduction of the electrode. The open-circuit voltage of the device is slightly above 0.7 V.

The output characteristics of eight pairs of Bi_2Te_3-based devices are shown in Table 3. The conversion efficiency of Bi_2Te_3-based device before neutron irradiation is 5.88%. After irradiation, though thermoelectric properties of n-type $Bi_2Te_{2.7}Se_{0.3}$ and p-type $Bi_{0.5}Sb_{1.5}Te_3$ materials vary, the output power and efficiency of devices are practically stable, which is due to the decrease in the properties of p-type $Bi_{0.5}Sb_{1.5}Te_3$ material offset by the increase of n-type $Bi_2Te_{2.7}Se_{0.3}$ materials. Interestingly, if we only irradiated the n-type $Bi_2Te_{2.7}Se_{0.3}$ material with targeted neutrons and left the p-type $Bi_{0.5}Sb_{1.5}Te_3$ material untreated, then the conversion efficiency of the combined TE device could be increased to 6.53%. This result is somewhat of an overturning of our previous knowledge, and may be an effective means to drive further development of thermoelectric energy conversion technology. In addition, the TE devices compensate and recover during the actual service, thereby prolonging its working time. Moreover, we can pre-treat the n-type material by irradiating it with neutrons before welding and forming the device to enhance its overall output properties.

4. Conclusion

We successfully prepared the bulk n-type $Bi_2Te_{2.7}Se_{0.3}$ and p-type $Bi_{0.5}Sb_{1.5}Te_3$ materials based on cold pressing and molding and irradiated them at a pulsed reactor with a neutron fluence of 4.56×10^{10} and 1×10^{13} n/cm^2. After irradiation, in n-type $Bi_2Te_{2.7}Se_{0.3}$ materials, the carrier concentration decreases, and the hall mobility increases, which primarily enhances the electrical conductivity and promotes the maximum ZT value from 0.80 to 1.07. Moreover, the circumstance of p-type $Bi_{0.5}Sb_{1.5}Te_3$ materials is completely opposite to the n-type, which makes its average ZT values decrease 10.4% and 19.9%. The output of thermoelectric legs is simulated by the finite-element simulation performed for thermoelectric single legs. The maximum evaluated efficiency reaches 6.81% for n-type $Bi_2Te_{2.7}Se_{0.3}$ and 6.25% for p-type $Bi_{0.5}Sb_{1.5}Te_3$ at the temperature difference of $\Delta T = 250$ K. When n-type $Bi_2Te_{2.7}Se_{0.3}$ and p-type $Bi_{0.5}Sb_{1.5}Te_3$ materials form eight pairs of Bi_2Te_3-based devices, the conversion efficiency without irradiation is 5.88%, which fluctuates slightly to 5.91%, and 5.94% after irradiation which means that in RTG, the effect of neutron irradiation to Bi_2Te_3-based TE devices is infinitesimally small. Given the enhancement of the properties of the n-type $Bi_2Te_{2.7}Se_{0.3}$ material by neutron irradiation, we can maintain this enhancement while reducing the degradation of the performance of the p-type $Bi_{0.5}Sb_{1.5}Te_3$ material through measures such as radiation hardening to enhance the output power and conversion efficiency of Bi_2Te_3-based TE devices and combine them with medium and high-temperature thermoelectric materials to improve the overall conversion efficiency of the device. In other applications of thermoelectric devices, such as recovering waste heat and reducing carbon emissions, neutron irradiation can used as a modification method to improve the performance of n-type $Bi_2Te_{2.7}Se_{0.3}$ thermoelectric materials for obtaining a better economic efficiency. A fly in the ointment is that the COMSOL simulation ignores the current loss caused by the contact resistance and the temperature reduction on the ceramic plate, indicating differences between simulation and experimental results. However, the existing results show that the gap between the simulation and experiment is small. Thus, our results are still of referential significance. Nevertheless, the effects of neutron irradiation must be experimentally evaluated, which is the direction of our next work.

Declaration of competing interest

The authors declare that they have no known competing financial interests or personal relationships that could have appeared to influence the work reported in this paper.

Acknowledgments

This work is supported by the Ministry of Science and Technology Foreign Expert Project (Grant No. G2022181007L), the Shanghai Aerospace Science and Technology Innovation Project (Grant No. SAST2020-097), and the Excellent Postdoctoral Program of Jiangsu Province (Grant No. 2022ZB235).

References

[1] Y. Xing, R. Liu, J. Liao, et al., A device-to-material strategy guiding the "double-high" thermoelectric module, Joule 4 (11) (2020) 2475–2483.
[2] G. Wang, R. Hu, H. Wei, et al., The effect of temperature changes on electrical performance of the betavoltaic cell, Appl. Radiat. Isot. 68 (12) (2010) 2214–2217.
[3] H. Williams, R. Ambrosi, N. Bannister, et al., A conceptual spacecraft radioisotope thermoelectric and heating unit (RTHU), Int. J. Energy Res. 36 (12) (2012) 1192–1200.
[4] A Chmielewski, RTGs for space exploration at the end of the 20th century[C]/. Proceedings of the 24th Intersociety Energy Conversion Engineering Conference, 1989, pp. 715-720.
[5] S.A. Whalen, C.A. Apblett, T.L. Aselage, Improving power density and efficiency of miniature radioisotopic thermoelectric generators, J. Power Sources 180 (1) (2008) 657–663.
[6] Y. Ma, J. Liu, H. Yu, et al., Coupled irradiation-thermal-mechanical analysis of the solid-state core in a heat pipe cooled reactor, Nucl. Eng. Technol. 54 (6) (2022) 2094–2106.
[7] I.L.A. Daryush, Thermoelectric systems: ion beam enhanced thermoelectric properties, Appl. Surf. Sci. 310 (2014) 217–220.
[8] N. Kempf, C. Karthik, B.J. Jaques, et al., Proton irradiation effect on thermoelectric properties of nanostructured n-type half-Heusler $Hf_{0.25}Zr_{0.75}NiSn_{0.99}Sb_{0.01}$, Appl. Phys. Lett. 112 (2018), 243902.
[9] J.W. Vandersande, J. Mccormack, A. Zoltan, et al., Effect of neutron irradiation on the thermoelectric properties of SiGe alloys, Solid State Phys. 2 (1990) 392–396.
[10] P. Ballo, P. Macko, L. Harmatha, et al., Thermoelectrical parameters of fast

neutron irradiated GeSi alloys, Phys. Status Solidi 150 (2) (2010) 687–693.
[11] H. Wang, K.J. Leonard, Effect of high fluence neutron irradiation on transport properties of thermoelectrics, Appl. Phys. Lett. 111 (4) (2017), 49301.
[12] L.V. Gorynin, V.A. Ignatov, V.V. Rybin, Effects of neutron irradiation on properties of refractory metals, J. Nucl. Mater. 191 (1992) 421–425.
[13] S.A. Fabritsiev, V.A. Gosudarenkova, V.A. Potapova, et al., Effects of neutron irradiation on physical and mechanical properties of Mo-Re alloys, J. Nucl. Mater. 191 (1992) 426–429.
[14] T. Koyanagi, Y. Katoh, K. Ozawa, et al., Neutron-irradiation creep of silicon carbide materials beyond the initial transient, J. Nucl. Mater. 478 (2016) 97–111.
[15] E. Huseynov, A. Garibov, R. Mehdiyeva, et al., Effects of neutron flux, frequency and temperature on the dielectric loss of nano SiO_2 particles, Silicon 10 (2) (2018) 191–196.
[16] E. Huseynov, A. Jazbec, L. Snoj, Temperature vs. impedance dependencies of neutron-irradiated nanocrystalline silicon carbide (3C-SiC), Appl. Phys. A 125 (2019) 91–98.
[17] E. Huseynov, A. Garibov, R. Mehdiyeva, Temperature and frequency dependence of electric conductivity in nano-grained SiO_2 exposed to neutron irradiation, Physica B 450 (2014) 77–83.
[18] L.L. Snead, T. Nozawa, Y. Katoh, et al., Handbook of SiC properties for fuel performance modeling, J. Nucl. Mater. 371 (2007) 329–377.
[19] V. Barabash, G. Federici, M. Rodig, et al., Neutron irradiation effects on plasma facing materials, J. Nucl. Mater. 283 (2000) 138–146.
[20] L.L. Snead, Limits on irradiation-induced thermal conductivity and electrical resistivity in silicon carbide materials, J. Nucl. Mater. 329 (2004) 524–529.
[21] E.M. Huseynov, Electrical impedance spectroscopy of neutron-irradiated nanocrystalline silicon carbide (3C-SiC), Appl. Phys. A 124 (2018) 19.
[22] E.M. Huseynov, Dielectric loss of neutron-irradiated nanocrystalline silicon carbide (3C-SiC) as a function of frequency and temperature, Solid State Sci. 84 (2018) 44–50.
[23] E.M. Huseynov, Neutron irradiation and frequency effects on the electrical conductivity of nanocrystalline silicon carbide (3C-SiC), Phys. Lett. 380 (38) (2016) 3086–3091.
[24] C. Wang, X. Jin, W. Chen, et al., The impact of reactor neutron irradiation on total ionizing dose degradation in MOSFET, Nucl. Instrum. Methods Phys. Res. Sect. A Accel. Spectrom. Detect. Assoc. Equip. 924 (21) (2019) 245–249.
[25] K. Liu, X. Tang, Y. Liu, et al., Enhancing the performance of fully-scaled structure-adjustable 3D thermoelectric devices based on cold–press sintering and molding, Energy 206 (2020), 118096.
[26] M. Maksymuk, B. Dzundza, O. Matkivsky, et al., Development of the high performance thermoelectric unicouple based on Bi_2Te_3 compounds, J. Power Sources 530 (2022), 231301.
[27] G.J. Snyder, E.S. Toberer, Complex thermoelectric materials, Nat. Mater. 7 (2008) 105–114.
[28] M.S. Dresselhaus, M.Y. Tang, et al., New directions for low–dimensional thermoelectric materials, Adv. Mater. 19 (8) (2007) 1043–1053.
[29] Z. Lin, H. Dang, C. Zhao, et al., The cross-interface energy-filtering effect at organic/inorganic interfaces balances the tradeoff between thermopower and conductivity, Nanoscale 14 (2022) 9419.
[30] M. Bala, R. Meena, S. Gupta, et al., Formation of nanodots and enhancement of thermoelectric power induced by ion irradiation in PbTe:Ag composite thin films, Nucl. Instrum. Methods Phys. Res. B 379 (2016) 36–41.
[31] F. Zhang, D. Wu, J. He, The roles of grain boundaries in thermoelectric transports, Materials Lab 1 (1) (2022), 220012.
[32] C. Uher, J. Yang, S. Hu, et al., Transport properties of pure and doped MniSn (M= Zr, Hf), Phys. Rev. B 59 (13) (1999) 8615–8621.
[33] Y. Li, J. Li, J. Du, et al., Response of p-type and n-type Half-Heusler thermoelectric materials to fast neutron irradiation, Nucl. Instrum. Methods Phys. Res. Sect. B Beam Interact. Mater. Atoms 479 (2020) 55–67.
[34] C. Hu, K. Xia, C. Fu, et al., Carrier grain boundary scattering in thermoelectric materials, Energy Environ. Sci. 15 (2022) 1406.
[35] C.M. Barr, E.Y. Chen, J.E. Nathaniel II, et al., Irradiation-induced grain boundary facet motion: in situ observations and atomic-scale mechanisms, Sci. Adv. 8 (23) (2022), eabn0900.
[36] X. Zheng, L. Zhu, Y. Zhou, et al., Impact of grain sizes on phonon thermal conductivity of bulk thermoelectric materials, Appl. Phys. Lett. 87 (2005), 242101.
[37] E. Macía, A. García-Junceda, M. Serrano, et al., Effect of mechanical alloying on the microstructural evolution of a ferritic ODS steel with (Y–Ti–Al–Zr) addition processed by Spark Plasma Sintering (SPS), Nucl. Eng. Technol. 53 (8) (2021) 2582–2590.
[38] E. Papynov, A. Belov, O. Shichalin, et al., $SrAl_2Si_2O_8$ ceramic matrices for ^{90}Sr immobilization obtained via spark plasma sintering-reactive synthesis, Nucl. Eng. Technol. 53 (7) (2021) 2289–2294.
[39] C. Tang, D. Liang, H. Li, et al., Preparation and thermoelectric properties of $Cu_{1.8}S/CuSbS_2$ composites, J. Adv. Ceram. 8 (2019) 209–217.
[40] J. Ahn, G. Kim, Y. Jung, et al., Fabrication and thermal conductivity of CeO_2–Ce_3Si_2 composite, Nucl. Eng. Technol. 53 (2) (2021) 583–591.
[41] K. Park, S. Shin, A. Tazebay, et al., Lossless hybridization between photovoltaic and thermoelectric devices, Sci. Rep. 3 (2013) 2123.